The Astrophysical Journal, 608:601–609, 2004 June 10

OXYGEN/HYDROGEN CHEMISTRY IN THE INNER COMAE OF ACTIVE COMETS

Robert J. Glinski,[1] Brian J. Ford,[1] Walter M. Harris,[2] Christopher M. Anderson,[2] and Jeffery P. Morgenthaler[3]

Received 2003 February 3; accepted 2003 September 9

ABSTRACT

We have constructed a concentric-shell, one-dimensional kinetic model that examines the chemistry of hydrogen and oxygen species in detail. We have studied the effects of the reactions of the reactive OH, $O(^3P)$, and $O(^1D)$ species with themselves and with the abundant stable molecules in the inner coma of moderately and highly active comets. We find that the reactions (1) $O(^1D) + H_2O \rightarrow 2OH$ and (2) $O(^3P) + OH \rightarrow O_2 + H$ play important roles in the inner comae of active comets. Inclusion of reaction (2) predicts the formation of significant amounts of molecular oxygen. As the densities of O_2 may be as high as 1% those of water in some cases, the possibility of detection exists. We suggest the possibility that the ion O_2^+ may contribute to some previously unassigned features in the optical ion-tail spectra of comets. We also consider the role that reactions of the reactive species might play in the destruction of CO, NH_3, and organic molecules in the inner coma of the active comet. We find that destruction of formaldehyde, for example, by reaction with OH has a small but essentially negligible effect on the predicted production rate of formaldehyde. Finally, we examine the significance of the reaction of OH with CO in the dense inner coma.

Subject headings: astrochemistry — comets: general

1. INTRODUCTION

The recent appearance of the very bright comet Hale-Bopp (C/1995 O1) has created an unprecedented opportunity to study a comet with a dense and extended collision zone. The activity of the nucleus caused the number densities of many of the gas-phase constituents to be quite high for comets. Near perihelion, the OH and O atom number densities were on the order of 10^6 and 10^5 cm^{-3}, respectively, at about 10^4 km from the nucleus. In addition, the residence time of a reactive species in the collision zone, which extended to about 3×10^5 km near perihelion, was as high as 3×10^5 s (Harris et al. 2002). This implies that bimolecular reactions of neutral species may be significant in comets as active as Hale-Bopp. Detailed chemical modeling (Rodgers & Charnley 2001a) has shown that chemical reactions in the coma are probably insufficient for producing some newly observed organic molecules (Bockelée-Morvan et al. 2000). But gas-phase chemistry could be of use in understanding some of the observations of the deuterium chemistry, including the HNC/HCN ratio (Rodgers & Charnley 2001b, 2002).

Although the organic chemistry is becoming better understood, we sought to focus on the detailed chemistry of water and its photodissociation products. From reading the literature, we noted that several key hydrogen/oxygen reactions were often neglected. Following the suggestions of Komitov (1989) and Budzien, et al. (1994), we have explored the extent to which reactions of the photodissociation products of water affect the overall oxygen/hydrogen chemistry in the inner coma. We have constructed a photochemical kinetic model of the inner coma that focuses on several relatively fast bimolecular reactions. We used this model to study in detail the reactions of $O(^1D)$, $O(^3P)$, and OH. We were especially interested in the roles played by the reactions

$$O(^1D) + H_2O \rightarrow 2OH, \quad (1)$$

$$O(^3P) + OH \rightarrow O_2 + H. \quad (2)$$

The model calculates the one-dimensional distributions of the oxygen/hydrogen species for highly active comets such as Hale-Bopp and other moderately active comets. The inclusion of reaction (2) suggests that O_2 may be a minor constituent in some comets and that it might be detected as the ion O_2^+.

The relatively high number densities of the radical species compelled us to investigate the effects of reactive collisions of these with CO and several select organic molecules. We specifically examined the reactions

$$OH + CH_2O \rightarrow HCO + H_2O \quad (3)$$

and

$$OH + CO \rightarrow CO_2 + H. \quad (4)$$

Although these reactions slightly reduce the densities of CO and CH_2O, we found no reason to revise upward the production rates of these species due to chemical reaction losses in the inner coma. In addition, the presence of carbon-containing species had only a slight effect on the concentrations of the oxygen/hydrogen species.

2. DESCRIPTION OF THE MODEL

We have sought to examine the chemistry in the inner coma using relatively well established physical properties of the comet atmosphere, i.e., the temperature, velocity, and water density structure (Combi & Delsemme 1980; Festou 1981a,

[1] Department of Chemistry, Tennessee Technological University, Cookeville, TN 38505; rglinski@tntech.edu.
[2] Department of Astronomy, University of Wisconsin, Madison, WI 53706.
[3] NASA Goddard Space Flight Center, Code 681, Greenbelt, MD 20771.

1981b; Combi & Smyth 1988a, 1988b; Rodgers & Charnley 2002). Our model divides the coma into 14 shells centered on the nucleus; the innermost shell is bounded at 200 km from the center. Each subsequent shell's outer boundary was twice as far as that of the previous shell; hence, the outer boundary of the final shell was at 1,638,400 km. The initial composition of the gas was assumed to be water and proportionate amounts of the other parent molecules, e.g., CO, CO_2, and CH_2O. The initial volume densities were calculated from the known production rates and the radial flow velocity at the midpoint of the first shell, 100 km. Starting with the parent molecules, the photochemical kinetic model was run for the residence time in the first shell. The concentrations at the end of that time were diluted by the appropriate factor and entered as the initial conditions for the next shell, and the process was repeated. Absolute volume densities were thereby obtained for all the shells referenced to the midpoint of the shell. Column densities were calculated by integrating the volume densities along chords drawn at arbitrarily chosen projected distances from the nucleus, ranging from $r_c = 1 \times 10^3$ to 3×10^5 km.

A reaction set was constructed that included all the photodissociation pathways and the significant bimolecular reactions. The mechanism studied is listed in Table 1. The chemical kinetics were followed explicitly by solution of the coupled, time-dependent differential equations for all the species. The software package, which employs the Gear subroutine, has been described previously (Braun et al. 1988; Glinski et al. 2001). All loss processes due to photoionization were included, but the total ion chemistry was not considered in the model. Comprehensive magnetohydrodynamic (MHD) modeling, such as that done by Schmidt et al. (1988) or Wegmann, Jockers, & Bonev (1999), was not attempted. To justify this, we performed an approximate modeling of the system including the ion chemistry mechanism shown in Rauer (1999). We found that inclusion of all reactions containing an ion (or a carbon atom) as a reactant resulted in a negligible change to the calculated column density of any oxygen or hydrogen species inside of 5×10^5 km.

The gas in each shell was characterized by a radial velocity vector, kinetic temperature, and an attenuation factor for the solar flux. Figure 1 shows the expansion velocities and temperature for each cell adopted from previous modeling studies, which included hydrodynamics. The expansion velocities for the most active comet model, similar to Hale-Bopp model near perihelion, were taken directly from the models of Combi et al. (1999, 2000). For the less active comets, velocity structures having less acceleration were deduced from the work of Combi (1989, 1996) and Combi et al. (1999) and are also consistent with those of Rodgers & Charnley (2002). From these published models we could also deduce a reasonable temperature distribution in the inner comae. It was important to realize that the reactions of interest here are moderately temperature dependent and that it is the relative kinetic temperature of OH with the reaction partner that had to be considered. Reactions (2), (3), and (4) are relatively slow, however, and both $O(^3P)$ and OH will collide many times with a water molecule before reacting. Therefore, even though $O(^3P)$ and OH are products of exothermic reactions, their kinetic temperatures should be similar to that of water in the collisional coma. Using the results of Combi (1996) as a guide, we could estimate the temperature profiles shown in Figure 1. We also fixed the minimum temperature in the two models for the comets with the lower production rates to 45 K, in order to keep the rates of reactions (2) and (3) from becoming nonphysically fast. As a check of the overall sensitivity of the model to temperature profile, models were run using an average temperature of 90 K throughout the coma. This is roughly the rotational temperature of CO (DiSanti et al. 1997, 2001) and H_2O (Dello Russo et al. 2000) in the collisional coma of Hale-Bopp. We found that densities of the oxygen atoms and OH were insignificantly different than when a nonconstant temperature profile was used. The predicted O_2 densities were, however, significantly different, and these temperature effects are discussed below.

As the inner shells of each model can become optically thick at the wavelengths where water and CO absorb, we attenuated the solar flux in an appropriate manner. We divided the far UV into three regions: less than 100 nm, from 100 to 185 nm, and at the wavelength of Lyα, 121.6 nm. The attenuation factors for each shell reflected the average absorption cross section of water or CO at these wavelengths and the summed column density of water or CO in the outer shells, which were obtained from a model run without attenuation. The average cross sections of water were estimated from Watanabe & Zelikoff (1953), Watanabe & Jursa (1964), and the Center for Astrophysics database[4] as 1.8×10^{-17}, 3.5×10^{-18}, and 1.4×10^{-17} cm^2, respectively, for the wavelength regions above. For CO, an average cross section of 2.0×10^{-17} cm^2 was used for wavelengths below 100 nm (Henry & McElroy 1968). These attenuation factors were applied to the photorates in proportions deduced for each photodissociation route from the tables of Heubner et al. (1992).

We do not expect that our model yields good predictions of column densities beyond about $r_c = 4 \times 10^5$ km, for several reasons. We have made the last shell bounded and do not expand the gas to infinity. Beyond the collision zone the chosen kinetic temperature becomes a poor estimate of the collision energy of the reactions of interest, although at the same time collisions become less important. In addition, the products of CO and CO_2 photolysis become increasingly important beyond that radius, as do complex ion chemistry and solar wind driven processes. The effects of an accelerated velocity distribution on the density profile of OH at larger radii have been investigated in a recent paper by Harris et al. (2002). We also assume that there is no molecule production from the dust.

The goal of this modeling was to obtain a reasonably accurate description of the composition of the inner coma, $r_c = 1 \times 10^3$ to 4×10^5 km, where some data on the $O(^1D)$ and OH column densities exist for comparison. The model could be tested against data from Hale-Bopp when it was at a heliocentric distance of about 1 AU pre-perihelion and when the water production rate was between 0.7 and 1.0×10^{31} molecules s^{-1} (Combi et al. 2000; Dello Russo et al. 2000). The $O(^1D)$ and OH data discussed here were taken from observations of Hale-Bopp described previously (Morgenthaler et al. 2001). The calculated column densities were converted to surface brightness to compare to the observations. For OH, the surface brightness in Rayleighs was calculated as $10^{-6} N_{\rm OH} g_{\rm OH}$, where $N_{\rm OH}$ is the column density in cm^{-2} and $g_{\rm OH}$ is the fluorescence efficiency, taken to be 2.5×10^{-4} photons s^{-1} molecule^{-1} on the date of the OH observations (Schleicher & A'Hearn 1982, 1988). The $O(^1D)$ surface brightness was calculated as $10^{-6} N_{O(^1D)} \tau^{-1}$, where τ^{-1} is the decay rate of the prompt emission, 0.00563 s^{-1}, going into the 6300 Å line that was measured.[5]

[4] See http://cfa-www.harvard.edu/amdata/ampdata/VUV_H2O/.
[5] See http://physics.nist.gov/cgi-bin/AtData/main_asd.

TABLE 1

RATE CONSTANTS USED IN THIS MODELING

Reaction No.	Reaction	k (s^{-1})	k (cm^3 $molecule^{-1}$ s^{-1})	Source	Notes
1*.....	$O(^1D) + H_2O \rightarrow OH + OH$		2.1E−10	[a]	$E_a = 0$
2*.....	$O(^3P) + OH \rightarrow O_2 + H$		2.4E−11($e^{+110/T}$)	[a]	UMIST: 1.8E−11($e^{+178/T}$)
3*.....	$OH + CH_2O \rightarrow$ products		8.2E−12($e^{+40/T}$)	[a]	
4*.....	$OH + CO \rightarrow CO_2 + H$		2.8E−13($e^{-176/T}$)	[a, b]	UMIST: 1.2E−11(T/300)$^{0.95}$($e^{+74/T}$)
5*.....	$OH \rightarrow O(^3P) + H$	(8.6 ± 2.0)E−6		This paper	
6*.....	$OH \rightarrow O(^1D) + H$	(2.1 ± 1.0)E−6		This paper	
7.....	$H_2O \rightarrow H + OH$	1.03E−5		[c]	
8.....	$H_2O \rightarrow H_2 + O(^1D)$	5.97E−7		[c]	
9.....	$H_2O \rightarrow H + H + O(^3P)$	7.55E−7		[c]	
10.....	$H_2 \rightarrow H + H$	8.2E−8		[c]	
11.....	$O_2 \rightarrow O(^3P) + O(^1D)$	4.1E−6		[c]	
12.....	$O(^1D) + H_2O \rightarrow O(^3P) + H_2O$		9.0E−12	[a]	$E_a = 0$
13.....	$O(^1D) + H_2O \rightarrow H_2 + O_2$		2.2E−12	[a]	$E_a = 0$
14.....	$O(^1D) + OH \rightarrow O_2 + H$		1.0E−10	[a]	$E_a = 0$
15.....	$O(^1D) + H_2 \rightarrow OH + H$		1.1E−10	[a]	$E_a = 0$
16.....	$OH + OH \rightarrow H_2O + O(^3P)$		3.9E−13(T/300)$^{1.69}$($e^{+57/T}$)	[a]	UMIST
17.....	$O(^1D) \rightarrow O(^3P)$	7.5E−3		[d]	
21.....	$CO \rightarrow C + O(^3P)$	2.8E−7		[c]	
22.....	$CO \rightarrow C + O(^1D)$	3.5E−8		[c]	
23.....	$CO \rightarrow CO^+ + e^-$	3.8E−7		[c]	
24.....	$CO_2 \rightarrow CO + O(^1D)$	9.2E−7		[c]	
25.....	$CO_2 \rightarrow CO + O(^3P)$	3.0E−7		[c]	
26.....	$CO_2 \rightarrow CO_2 + e^-$	6.5E−7		[c]	
31.....	$O(^1D) + CO \rightarrow O(^3P) + CO$		4.7E−11$e^{-64/T}$	[a]	
32.....	$O(^1D) + CO \rightarrow CO_2$		8.0E−11	[a]	$E_a = 0$
33.....	$O(^1D) + CO_2 \rightarrow O(^3P) + CO_2$		7.4E−11$e^{-120/T}$	[a]	
34.....	$O(^1D) + CO_2 \rightarrow CO + O_2$		2.0E−10	[a]	$E_a = 0$
35.....	$C + O_2 \rightarrow CO + O(^3P)$		2.0E−11	[a]	$E_a = 0$
41.....	$CH_2O \rightarrow$ products	2.1E−4		[a]	
42.....	$O(^1D) + CH_2O \rightarrow$ products		2.0E−10	[a]	$E_a = 0$
51.....	$H_2O \rightarrow H_2O^+ + e^-$	3.3E−7		[c]	
52.....	$H_2O \rightarrow OH^+ + H + e^-$	5.5E−8		[c]	
53.....	$OH \rightarrow OH^+ + e^-$	2.5E−7		[c]	
54.....	$O_2 \rightarrow O_2^+ + e^-$	4.6E−7		[c]	
55.....	$O(^3P) \rightarrow O^+ + e^-$	2.1E−7		[c]	

NOTE.—Initial conditions are discussed in text. Asterisk indicates reaction discussed in text.

[a] Atkinson et al. (1997) and Demore et al. (1997).

[b] The rate constant has been measured at 90 K by Frost et al. (1993) as 1.0×10^{-13}.

[c] All photorates are taken at 1 AU, for a quiet Sun, from Heubner et al. (1992), except reactions (5) and (6).

[d] NIST Atomic Spectra Database (http://physics.nist.gov/cgi-bin/AtData/main_asd).

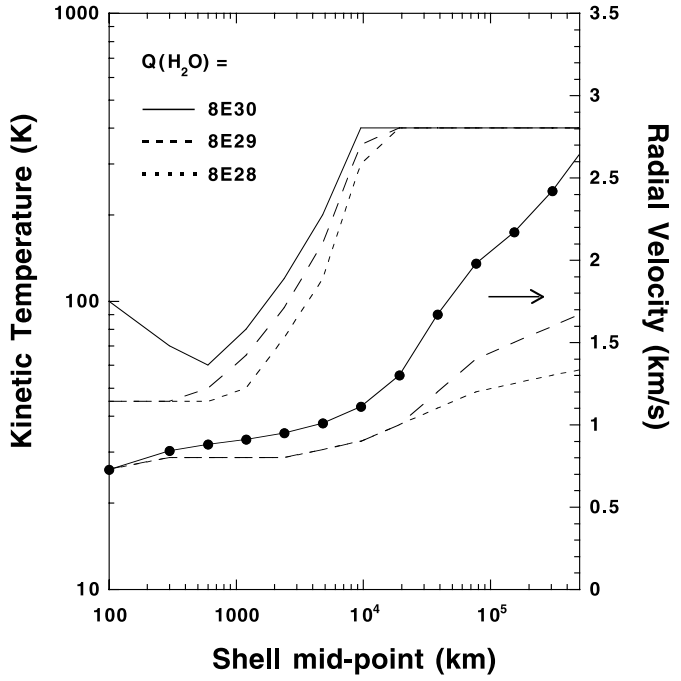

FIG. 1.—Kinetic temperature and radial velocity profiles for comets of three different activities considered in this modeling.

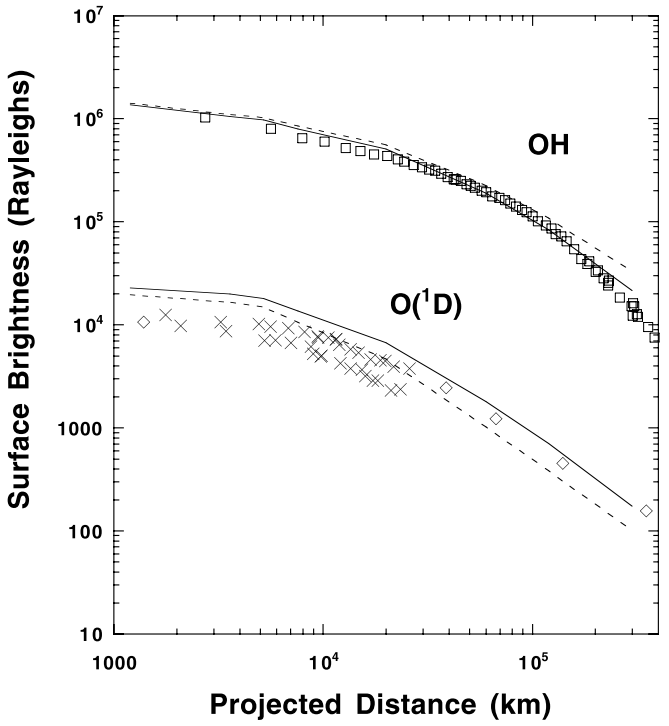

FIG. 2.—Comparison of observed and modeled surface brightnesses of OH and O(^1D) for comet Hale-Bopp near perihelion; $Q(H_2O) = 9.1 \times 10^{30}$ molecules s^{-1} and $R_h = 0.94$ AU. Solid lines are the model results using the rate constants in Table 1. Dotted lines are the same, except that the photorates for OH of van Dishoeck & Dalgarno (1984) were used. *Squares*, 1997 March 28; *open diamonds*, March 16; crosses, March 18 (Morgenthaler et al. 2001).

The OH data shown below were taken on 1997 March 28 and the O(^1D) data were taken on March 16 and 18 (Morgenthaler et al. 2001). The model used to compare with the Hale-Bopp data corresponded to conditions interpolated on the intermediate date, March 23. Specifically, this was run for a heliocentric distance of 0.94 AU and a water production rate of 9.1×10^{30} molecules s^{-1}. We believe it was justified to compare this model result to the data taken on different days, since the day-to-day variability of the water production rate was as much as 10% in the 2 weeks pre-perihelion (Combi et al. 2000). This model also used the temperature and radial velocity profiles shown in Figure 1 for the comet of highest activity. We show the results of this comparison below. The contributions of bimolecular reactions was explored using models for comets at 1.0 AU, which have water production rates of 8×10^{30}, 8×10^{29}, and 8×10^{28} molecules s^{-1}.

3. MODELING RESULTS

3.1. *Reactions of* O *and* OH

As explored in a previous paper (Morgenthaler et al. 2001), the uncertain factors that control the predicted OH and O(^1D) densities are reaction (1) and the values of the photodissociation rate constants of the two OH photolysis pathways,

$$\mathrm{OH} + \mathrm{photon} \rightarrow \mathrm{O}(^1P) + \mathrm{H}, \quad (5)$$

$$\rightarrow O(^1D) + \mathrm{H}. \quad (6)$$

In that paper, it was difficult to fit the OH and O(^1D) column densities in Hale-Bopp consistently for a particular choice of rates of reactions (5) and (6) when the products of reaction (1) were neglected. The results of our new Hale-Bopp comparison model that includes chemical reactions are shown in Figure 2.

The solid lines in Figure 2 are for the values of the photorates for reactions (5) and (6) listed in Table 1 as 8.6×10^{-6} and 2.1×10^{-6} s^{-1} for production of O(^3P) and O(^1D), respectively. These were chosen because they corresponded to the best simultaneous fit of the OH and O(^1D) data between 4×10^4 and 4×10^5 km. Also shown in Figure 2 are the model results using the theoretical photorates of van Dishoeck & Dalgarno (1984), 6.5×10^{-6} and 6.3×10^{-7} s^{-1}, respectively. Use of those values leads to a slight overprediction of OH and underprediction of O(^1D) beyond near 10^5 km. But it is seen that the OH and O(^1D) column densities are relatively insensitive to the OH photorates; hence, the problematic branching ratios of reactions (5) and (6) are not well constrained by this modeling. The chemical model can fit the observed OH and O(^1D) profiles reasonably well, although the O(^1D) may be somewhat overpredicted in the inner shells of the coma. The source of O(^1D) in the inner coma is predominately the photodissociation of water at Lyα; but we did not investigate the effects of this photorate, the branching ratios, or the variability of solar Lyα.

Having made our best fit of the photorates for reactions (5) and (6), we could explore the importance of reactions (1) and (2) in the coma. The results of this modeling are shown in Figure 3 for comets having water production rates of 8×10^{30}, 8×10^{29}, and 8×10^{28} s^{-1} at 1 AU. Two sets of results are shown: results for the model that included all the reactions in Table 1, and results when the bimolecular reactions were omitted. It can be seen that failure to include the bimolecular reaction (1) leads to an overprediction of O(^1D) inside of 10^4 km in the most active comets. The effects of this reaction are negligible in comets having $Q(H_2O) < 10^{29}$ s^{-1}.

3.2. *Production of* O_2

This modeling of active comets led us to consider the production of the hitherto neglected molecular oxygen, O_2. The volume densities of $O(^3P)$ and OH are relatively high for any atmosphere (Yung & DeMore 1999), compelling us to take reaction (2) into account. Figure 3 shows the column density profiles of O_2 when reaction (2) is included. The results, for the complete models that include all of the O_2 production and destruction pathways, suggest that there is a moderate density of O_2 in active comets and a significant density in less active comets. In Table 2 we present our calculated ratios of the O_2 to H_2O densities and production rates for comets of three different activities. We note that the column density of O_2 may be as high as 1% that of H_2O at a 2×10^4 km projected distance from a highly active comet. These densities would make O_2 a moderately abundant constituent in the inner coma of an active comet and suggests that it might be detectable by some means. In addition, the O_2 is itself unreactive and the relatively slow photodissociation rate suggests that much of it survives to be photoionized. The potential for the detection of O_2 or O_2^+ is discussed below. Although reactions (13), (14), and (34) produce O_2, their contribution is slight, as would be the contribution of any other ion-molecule reaction not considered.

3.3. *Inclusion of* CO, CO_2, *and Organic Compounds*

In our modeling, we found that the presence of carbon-containing molecules had relatively little effect on the oxygen/hydrogen chemistry in the inner coma. This is reasonable, since most of the carbon-bearing species are either few in number or have reaction and photodissociation rates that are relatively slow, such as those for the principal species, CO. But realizing that the densities of the reactive species, OH and O, were relatively high, we sought to explore the effects of chemical reactions in the inner coma on CO, CO_2, and other constituents. It is well known that the reactions of OH and $O(^1D)$ with small hydrocarbons occur predominantly via hydrogen extraction, and some are relatively fast (Yung & DeMore 1999). We were compelled to ask how much of an organic compound might be lost to reaction before it escaped the collision zone of a highly active comet. Since molecules spent as long as 3×10^5 s in the collision zone of Hale-Bopp, we sought to examine whether these reactions were at all competitive with photodissociation. Destruction via chemical reaction could lead to an underestimation of the amount of an organic material produced by the nucleus. In Table 3 we present a comparison of the photodissociation rates to bimolecular reaction rates for some carbon-containing compounds and ammonia in a highly active comet. One can see from Table 3 that in almost all cases reaction with OH or $O(^1D)$ is not competitive with photolysis as the destruction pathway for the principal constituents of active comets. The two reactions that are competitive with photolysis, however, are

$$\mathrm{OH} + \mathrm{CH_2O} \rightarrow \mathrm{HCO} + \mathrm{H_2O} \qquad (3)$$

and

$$\mathrm{OH} + \mathrm{CO} \rightarrow \mathrm{CO_2} + \mathrm{H}. \qquad (4)$$

At 2000 km, the loss rate of formaldehyde due to reaction (3) is 3.9×10^{-5} s^{-1}, which is about one-fifth of the photolysis rate. We have modeled the column density profile of formaldehyde with reaction (3) both included and excluded. Figure 4 shows the volume densities predicted by our Hale-Bopp comparison model. It can be seen in Figure 4 that reaction of formaldehyde with OH results in an at most 10% reduction of the formaldehyde production rate observed in the coma over that actually produced by the nucleus. We can draw a similar conclusion for methane and methanol in their reactions with $O(^1D)$. As these are the strongest cases for a chemical effect, however, we do not

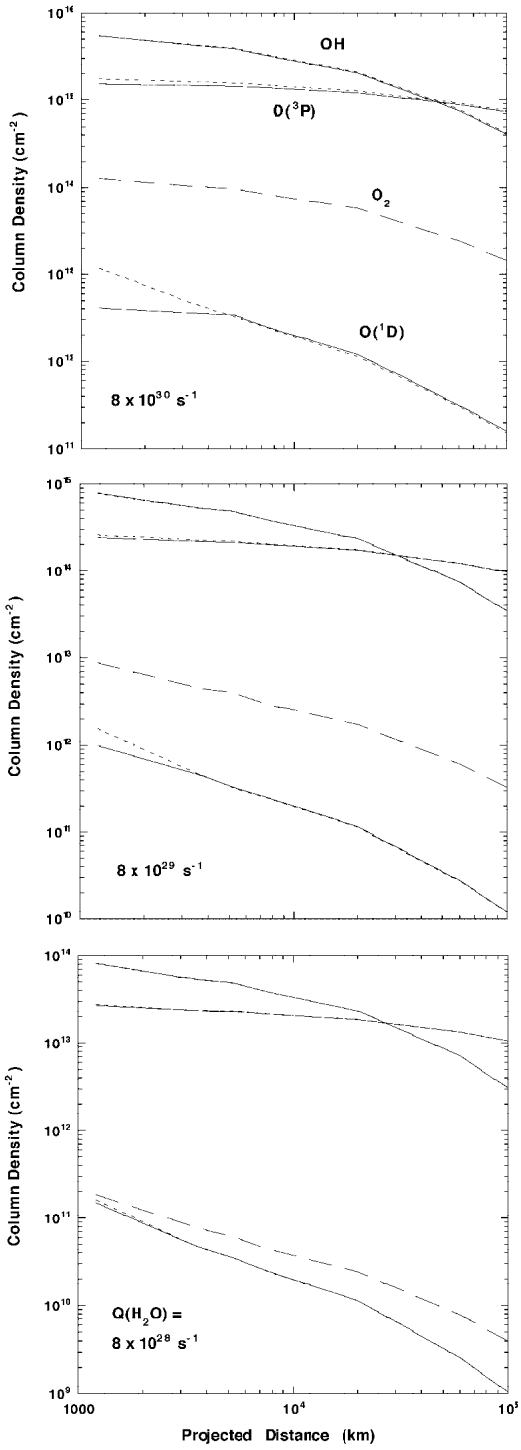

FIG. 3.—Predicted column densities for the model in Table 1, for comets exhibiting three different water production rates: 8×10^{30}, 8×10^{29}, and 8×10^{28} s^{-1}. Dotted lines are from the same model run but with the bimolecular reactions deleted. The O_2 densities are essentially zero when the reaction of O with OH is excluded.

TABLE 2
RATIOS OF O_2 TO H_2O PRODUCTION RATES AND COLUMN DENSITIES AT $r = 2 \times 10^4$ KM

	$Q(H_2O)$		
RATIO	8×10^{30}	8×10^{29}	8×10^{28}
$Q(O_2)/Q(H_2O)$	0.0036	0.0015	0.00023
$N(O_2)/N(H_2O)$	0.0091	0.0030	0.00044

NOTE.—Q = production rates (s^{-1}) calculated from the volume densities at 2×10^4 km; N = column densities (cm^{-2}) calculated at 2×10^4 km.

suggest the need to revise upward the production rates of the organic compounds, HCN, or NH_3 because of chemical losses in the coma of active comets. This supplements the results of Rodgers & Charnley (2001a), who found that homogeneous gas-phase chemistry probably does not contribute to the production of the organic molecules in the coma. It does not contribute to their loss, either.

It can be seen from Table 3 that at 2000 km the rate of loss of CO via reaction (4) is 3.9×10^{-7} s^{-1}, or about three-fifths of the photolysis rate. We therefore have also examined the effect of reaction of OH with CO on the CO profile. Upon running the model with and without reaction (4), we find that there is less than 2% difference in predicted CO production rate from the inner coma. This is smaller than the effect on formaldehyde, because the rates of reaction and photodissociation of CO are slow compared to those for formaldehyde. It is interesting to note that within about 1500 km of the nucleus, the rate of reaction of CO with OH, $k_{rxn} \times [OH]$, is greater than the rate of photolysis, k_{phot}, for a highly active comet. Another consequence is that reaction (4) is a small source of CO_2 in the inner coma. We calculate that the column density of the CO_2 produced by reaction (4) would be about 1% of that of "native" CO_2 if it were present in the nucleus at a fraction that is 0.02 times the water content.

4. DISCUSSION

We have constructed a relatively simple photochemical kinetic model that can describe the chemistry in the inner coma about as well as observational and laboratory kinetic data uncertainties allow. From this modeling we are led to the following conclusions:

1. The reaction $O(^1D) + H_2O \rightarrow 2OH$ (reaction [1]) is required to describe the composition of the inner coma of active comets. The reaction $O(^1D) + H_2O \rightarrow O(^3P) + H_2O$ does not occur for all practical purposes.
2. The reaction $O(^3P) + OH \rightarrow O_2 + H$ (reaction [2]) must be occurring in the inner coma of even moderately active comets and suggests that the usually neglected species, O_2, can have a significant density and may be detectable. Such a detection would be a strong indicator of bimolecular reactions in cometary atmospheres.
3. The fast hydrogen extraction reactions of OH and $O(^1D)$ with hydrocarbons, NH_3, or HCN are essentially negligible in affecting their densities.
4. The reaction of OH with CO is relatively insignificant to the oxygen/hydrogen chemistry, but it is the dominant loss process for CO in the dense inner coma and produces a small amount of CO_2.

Although our model is physically reasonable, it does contain the following assumptions: a spherical inner coma, a radial velocity vector that is the same for all species, and a kinetic temperature that is the same for all the neutrals *and* all the products. Considering these assumptions, our confidence in the results for the neutral species is raised by comparing our Figure 4 with the modeled density profiles resulting from

TABLE 3
COMPARISON OF PHOTOLYSIS RATES TO REACTION RATES FOR CARBON CONTAINING MOLECULES AND AMMONIA

		REACTION WITH OH		REACTION WITH $O(^1D)$	
SPECIES	PHOTO RATE (1 AU) (s^{-1})	k	k[OH] (s^{-1})	k	$k[O(^1D)]$ (s^{-1})
H_2O	1.2E−5	neg.	...	2.2E−10	4.4E−7
CH_4.....	3.6E−6	neg.	...	1.5E−10	3.0E−7
C_2H_6	1.1E−5	neg.	...	5.0E−10	1.0E−6
C_2H_2	1.3E−5	1.0E−14	3.5E−8	2.0E−10	4.0E−7
CH_2O.....	2.2E−4	1.1E−11	3.9E−5	2.0E−10	4.0E−7
CH_3OH.....	1.1E−5	8.0E−14	2.8E−7	5.0E−10	1.1E−6
NH_3	1.8E−4	neg.	...	2.5E−10	5.0E−7
HCN	1.3E−5	neg.	...	1.0E−10	2.0E−7
CO	6.5E−7	1.1E−13	3.9E−7	8.0E−11	1.6E−7
CO_2.....	2.0E−6	neg.	...	1.5E−10	3.0E−7

NOTES.—Rate constants are all at 90 K, and photo rates are for an unattenuated quiet Sun at 1 AU, taken from the references in Table 1; units of bimolecular rate constants are cm^3 $molecule^{-3}$ s^{-1}; number densities are those for the $Q_{water} = 8 \times 10^{30}$ molecule s^{-1} model, $n(OH) = 3.5 \times 10^6$ molecule cm^{-3} and $n(O(^1D)) = 2 \times 10^3$ molecule cm^{-3} at 2000 km; neg. means $k < 1 \times 10^{-14}$.

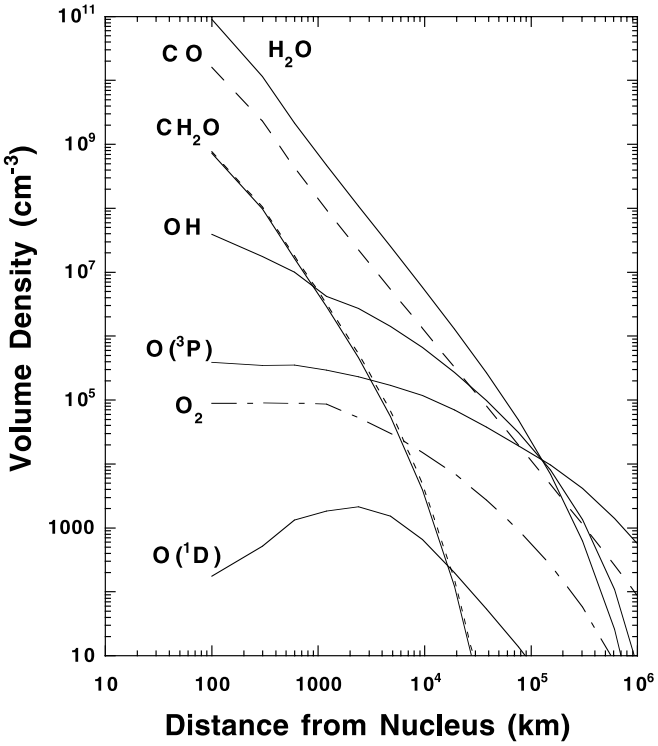

FIG. 4.—Predicted volume densities from the complete model, Table 1. Initial concentrations are the same as those used in the comparison model shown in Fig. 1 with 20% CO, 2% CO_2, and 1% CH_2O. For the formaldehyde traces, the solid line corresponds to the modeling result including both the bimolecular reaction, OH + CH_2O, and photodissociation; and the dotted line corresponds to the result when only photodissociation is included. Hence, a model that only includes photodissociation overpredicts the formaldehyde production rate only slightly.

Monte Carlo hydrodynamic modeling, partially including chemistry, shown in Combi (1996). Roughly the only difference between the volume densities of H_2O, OH, and O shown in Combi (1996) and in our Figure 4, between 2×10^3 and 1×10^5 km, is a factor of 10 increase in the Hale-Bopp densities over the Comet Halley densities. Indeed, many of our conclusions regarding the importance of bimolecular reactions can be deduced from the Combi figure scaled to the increased activity.

4.1. *Overall* O/H *Chemistry*

Although the physical quenching of $O(^1D)$ has been considered before (Festou & Feldman 1981; Morgenthaler et al. 2001), the key bimolecular chemical reactions of this study were reasonably left out of older studies, beginning with the seminal work of Giguere & Heubner (1978) and Heubner & Giguere (1980). At first approximation, there simply is not sufficient time for bimolecular reactions to have much of an effect on the production rate of H_2O or anything else. In later studies, Schmidt et al. (1988) and Wegmann et al. (1999) made comprehensive MHD studies of comets, including most of the bimolecular reactions used here. But in those, the effects of the reactions were not examined in detail, probably because of the expected insignificance of most of them in comets less active than the extraordinary Hale-Bopp.

In approaching the coma as a planetary atmosphere, we relied on the kinetics database used by atmospheric chemists (Yung & DeMore 1999), which drew our attention to the bimolecular reactions considered here. The rate constants in Table 1 are primarily from the NIST database, which includes the critical evaluations of DeMore et al. (1997)[6] and Atkinson et al. (1997). Some of the rate constants were checked with those in the comprehensive astrophysical UMIST rate file (Le Teuff, Millar, & Markwick 2000),[7] but there are some discrepancies between the two databases, as marked in Table 1. These differences, however, are probably not as great as the experimental uncertainties in some of the rate constants, which suggests the need for improved kinetics measurements of the key rate constants—especially below 200 K. Indeed, the choice of rate constant at temperatures less than about 200 K must be done quite cautiously in work of this nature.

Our rate constant of reaction (2) was taken from the evaluated list of Atkinson et al. (1997). That work gives a negative activation energy with a rather wide error limit, $E_a = -(915 \pm 831)$ J mol^{-1}. If the activation energy were actually in the high negative range, the production of O_2 would be lower in comets having higher coma temperatures. If the E_a were -1700 J mol^{-1}, for example, the rate constant would be only about one-fifth as fast at 300 K as at 90 K. On the other hand, the UMIST value of reaction (2) is several times faster than the NIST value at 90 K. For this reason our prediction of the O_2 density should be given wide error bars. If reaction (2) is indeed slower at high temperatures, it would be somewhat less important in Hale-Bopp than in other comets. It is possible that the O_2/H_2O ratio could be smaller for more active comets than the value shown in Table 2. In addition, the O_2/H_2O ratio in Hale-Bopp may have been proportionately larger at greater heliocentric distances than at 1 AU.

4.2. *Potential for the Detection of* O_2 *via* O_2^+ *Emission*

The predicted densities suggest that O_2 may be detectable in some manner. But this prospect is difficult for several reasons: the lack of a permanent dipole moment would rule out easy detection by vibrational or pure rotational spectroscopy, and the known electronic transitions occur in the difficult-to -study near-UV. However, the UV spectrum of comets has been relatively well characterized (Krishna Swamy 1997), and the several unidentified bands and lines are relatively weak. Therefore, any new emitter could only contribute a small fraction of the UV intensity. One possibility is that O_2 may appear as emission in the Herzberg ($A^3\Sigma_u^+ \rightarrow X^3\Sigma_g^-$) system. These are an extensive set of bands lying between 2500 and 4800 Å (Pearse & Gaydon 1976), which are, however, electric dipole forbidden (Krupenie 1972). Therefore, in comets this band system should be quite weak, as induced fluorescence is the expected excitation mechanism. In addition, the transition strength of this system would be spread over a large number of bands and lines, resulting in features being individually weak. Several other weak systems occur, but as they are seen it the air glow, they would be hard to detect in a cometary source (Pearse & Gaydon 1976).

As is the case for N_2 (Wyckoff & Theobald 1989; Cochran 2002), perhaps a better chance of detecting this molecule would be as the ion O_2^+. Since the ratio of the photoionization rate to the photodissociation rate is greater for O_2 than for H_2O, O_2^+ may be a relatively abundant ion. The ion has two well-studied transitions in optical and ultraviolet wavelengths. The second negative system ($A^2\Pi_u \rightarrow X^2\Pi_g$) lies in about the same region as the O_2 Herzberg bands (Pearse & Gaydon 1976). The first negative bands ($b^4\Sigma_g^- \rightarrow a^4\Pi_u$), however, lie in the visible region, and there is some hope of identifying these bands in

[6] Also available at http://kinetics.nist.gov/index.php.
[7] Also available at http://www.rate99.co.uk/.

TABLE 4
BAND HEADS AND BAND ORIGINS OF THE FIRST NEGATIVE SYSTEM ($b^4\Sigma_g^- - a^4\Pi_u$) OF O_2^+

Band ($v' - v''$)	Band Head[a] (Å)	Band Origin[b] (Å)	Franck-Condon Factor[c]
4–1	4998	4975.7	0.14
2–0	5295.7	5274.7	0.24
3–1	5274.7	5252.7	0.35
1–0	5631.9	5608.6	0.42
0–0	6026.4	5999.9	0.26
0–1	6418.7	6388.9	0.29
0–2	6856.3	6822.2	0.20

NOTE.—In the papers of Wyckoff et al. (1999) and Kawakita & Watanabe (2002), the unidentified lines and bands in plasma tail spectra fall in groups: 4917–5027, 5273–5339, 5605–5633, and 5991–6014 Å. Unassigned bands can be discerned on inspection of the plasma tail spectrum of Hale-Bopp (Rauer 1999) near 6380 and 6830 Å.

[a] Pearse & Gaydon (1976).
[b] Hansen et al. (1983).
[c] Jarmain et al. (1955).

comet spectra. Even if O_2^+ features were identified in comet spectra, they would need to be distinguished from any contribution from the terrestrial air glow, as was the issue with N_2^+ (Cochran 2002).

Recently, it has been noted that several unidentified, weak features show up in the plasma tail spectra of several comets (Wyckoff et al. 1999; Kawakita & Watanabe 2002). Two facts about their appearance are cogent: they appear to be associated with the water family of molecules, as opposed to the CO/CO_2 family, and they are relatively diminished in Hale-Bopp compared to less active comets. Our predicted O_2/H_2O density ratios in Table 2 are consistent with this. The O_2/H_2O ratio increases by a factor of about 10, going from a comet of activity 8×10^{28} s^{-1} to one of activity 8×10^{29} s^{-1}, but the O_2/H_2O ratio increases by a factor of only about 3, from a comet of activity 8×10^{29} s^{-1} to one of activity 8×10^{30} s^{-1}.

Table 4 lists the band origins and prominent band heads of the first negative series of O_2^+. As stated above, there are groups of unidentified lines in the optical spectra of plasma tails (Wyckoff et al. 1999; Kawakita & Watanabe 2002); these features appear clustered in groups near 4950, 5300, and 6000 Å. Our inspection of the plasma tail spectrum of Hale-Bopp (Rauer 1999) taken at 2.9 AU also seems to indicate unidentified features near 6380 and 6830 Å, which are not near H_2O^+ bands. There seems to be some coincidence of these groups with the band origins of the O_2^+ first negative bands. Since O_2 had been neither observed nor predicted in comets, Wyckoff et al. (1999) did not consider O_2^+ in their exhaustive list of candidates for the unidentified features. Although we do not suggest that all of these unidentified bands are due to O_2^+, we think that this modeling provides the grounds for considering it now.

A partial rotational analysis of several bands of the first negative system ($b^4\Sigma_g^- \rightarrow a^4\Pi_u$) O_2^+ emission spectrum has been presented by Nevin (1938, 1940). In that work the spectrum was obtained from an electric discharge of oxygen at about 1 torr. More recent work of Albritton et al. (1977) has shown that the rotational temperature of the O_2^+ in an electrodeless discharge is about 500 K, making it problematic to compare this laboratory spectrum to the comet spectrum. Presumably, the O_2^+ emission bands in space would reflect a radiative equilibrium, resulting in bands of different complexion than those observed in hot thermal sources. We have not attempted a complete analysis of this complex spectrum under the conditions of radiative equilibrium.

It has been shown previously (Glinski et al. 2001) that cometary molecules in radiative equilibrium will show a rotational population distribution that has two components. A generic molecule will display a hot distribution, caused by the radiation pumping, and a cold distribution, which may resemble the local thermal temperature. Although complex, the cometary O_2^+ spectrum may have some similarities to the spectrum of C_2. With no dipole moment, it might be expected that the excitation temperature of the hot component of O_2^+ (and O_2) would be quite high, but as in C_2 the band head due to the cold component would dominate (Krishna-Swami 1991a, 1991b, 1997; Glinski et al. 2001). We might expect that the strongest lines in an O_2^+ spectrum from space would have the strongest lines near the band origin. In addition, the transition probability of the entire electronic band is spread over a large number of vibrational and rotational transitions, especially since the bond distance of the two electronic states are quite different, as in C_2.

Although we do not suggest a mechanism for the ionization of O_2, it is plausible that the direct photoionization, $a^4\Pi_u \leftarrow X^3\Sigma_g^-$, yields the quartet ion states (Krupenie 1972). Clearly, if there is evidence of the O_2^+ first negative system, then there should be evidence for the second negative system or perhaps the O_2 Herzberg bands. However, these are in a difficult region of the near-UV to study, and we do not have access to such spectra.

It is also possible that the O_2^+ has already been detected in the in situ mass spectrometry experiments in the Comet Halley probes (Balsiger et al. 1986). In the work of Wegmann et al. (1987), their models slightly underpredicted the ion density for mass 32. Although they do include reaction (2) (Schmidt et al. 1988), they used a value of the rate constant that was only about 60% of that used here. They do not separate out the contributions from $^{32}S^+$ and $^{16}O_2^+$, however, so it was possible that a small O_2^+ signal may have been obscured by a larger $^{32}S^+$ peak in the mass spectrum.

This work was carried out under a NASA (OSS-01-PATM) grant to W. M. H. We thank Fred Zimmerman and Jesse Cates for their initial help with the kinetic and spectroscopic models.

REFERENCES

Albritton, D. L., Schmeltekopf, A. L., Harrop, W. J., Zare, R. N., & Czarny, J. 1977, J. Mol. Spectrosc., 67, 157
Atkinson, R., Baulch, D. L., Cox, R. A., Hampson, R. F., Jr., Kerr, J. A., Rossi, M. J., & Troe, J. 1997, J. Phys. Chem. Ref. Data, 26, 1329
Balsiger, H., et al. 1986, Nature, 321, 330
Bockelée-Morvan, D., et al. 2000, A&A, 353, 1101
Braun, W., Herron, J. T., & Kahaner, D. K. 1988, Int. J. Chem. Kinet., 20, 51
Budzien, S. A., Festou, M. C., & Feldman, P. D. 1994, Icarus, 107, 164
Cochran, A. L. 2002, ApJ, 576, L165
Combe, M. R., & Delsemme, A. H. 1980, ApJ, 237, 633
Combi, M. R. 1989, Icarus, 81, 41
———. 1996, Icarus, 123, 207
Combi, M. R., Cochran, A. L., Cochran, W. D., Lambert, D. L., & Johns-Krull, C. M. 1999, ApJ, 512, 961
Combi, M. R., Kabin, K., DeZeeuw, D. L., Gombosi, T. A., & Powell, K. G. 1999, Earth Moon Planets, 79, 275
Combi, M. R., Reinard, A. A., Bertaux, J.-L., Quemerais, E., & Mäkinen, T. 2000, Icarus, 144, 191
Combi, M. R., & Smyth, W. H. 1988a, ApJ, 327, 1026
———. 1988b, ApJ, 327, 1044
Dello Russo, N., Mumma, M. J., DiSanti, M. A., Magee-Sauer, K., Novak, R., & Rettig, T. W. 2000, Icarus, 143, 324
DeMore, W. B., et al. 1997, Chemical Kinetics and Photochemical Data for Use in Stratospheric Modeling. Evaluation Number 12 (JPL Publ. 97–4; Pasadena: JPL)
DiSanti, M. A., Mumma, M. J., Dello Russo, N., Magee-Sauer, K., Novak, R., & Rettig, T. W. 1997, Nature, 399, 662
———. 2001, Icarus, 153, 361
Festou, M. C. 1981a, A&A, 95, 69
———. 1981b, A&A, 96, 52
Festou, M. C., & Feldman, P. D. 1981, A&A, 103, 154
Frost, M. J., Sharkey, P., & Smith, I. W. M. 1993, J. Phys. Chem., 47, 12254
Giguere, P. T., & Huebner, W. F. 1978, ApJ, 223, 638
Glinski, R. J., Post, E. A., & Anderson, C. M. 2001, ApJ, 550, 1131
Hansen, J. C., Moseley, J. T., & Cosby, P. C. 1983, J. Mol. Spectrosc., 98, 48
Harris, W. M., Scherb, F., Mierkiewicz, E., Oliversen, R., & Morgenthaler, J. P. 2002, ApJ, 578, 996
Henry, R. J. W., & McElroy, M. B. 1968, in The Atmospheres of Venus and Mars, ed. J. C. Brandt & M. B. McElroy (New York: Gordon and Breach)
Huebner, W. F., & Giguere, P. T. 1980, ApJ, 238, 753
Huebner, W. F., Keady, J. J., & Lyon, S. P. 1992, Ap&SS, 195, 1
Jarmain, W. R., Fraser, P. A., & Nicholls, R. W. 1955, ApJ, 122, 55
Kawakita, H., & Watanabe, J. 2002, ApJ, 574, L183
Komitov, B. 1989, Adv. Space Res., 9, 177
Krishna Swamy, K. S. 1991a, ApJ, 373, 266
———. 1991b, Physics of Comets (Singapore: World Scientific)
———. 1997, ApJ, 481, 1004
Krupenie, P. H. 1972, J. Phys. Chem. Ref. Data, 1, 423
Le Teuff, Y. H., Millar, T. J., & Markwick, A. J. 2000, A&AS, 146, 157
Morgenthaler, J. P., et al. 2001, ApJ, 563, 451
Nevin, T. E. 1938, Philos. Trans. R. Soc. London A, 237, 471
———. 1940, Proc. R. Soc. London, 174, 371
Pearse, R. W. B., & Gaydon, A. G. 1976, The Identification of Molecular Spectra (4th Ed.; New York: Chapman Hall)
Rauer, H. 1999, Earth Moon Planets, 79, 161
Rodgers, S. D., & Charnley, S. B. 2001a, MNRAS, 320, L61
———. 2001b, MNRAS, 323, 84
———. 2002, MNRAS, 330, 660
Schleicher, D. G., & A'Hearn, M. F. 1982, ApJ, 258, 864
———. 1988, ApJ, 331, 1058
Schmidt, H. U., Wegmann, R., Huebner, W. F., & Boice, D. C. 1988, Comput. Phys. Commun., 49, 17
van Dishoeck, E. F., & Dalgarno, A. 1984, Icarus, 59, 305
Watanabe, K., & Jursa, A. S. 1964, J. Chem, Phys., 41, 1650
Watanabe, K., & Zelikoff, M. 1953, J. Opt. Soc. Am., 43, 753
Wegmann, R., Jockers, K., & Bonev, T. 1999, Planet. Space Sci., 47, 745
Wegmann, R., Schmidt, H. U., Huebner, W. F., & Boice, D. C. 1987, A&A, 187, 339
Wyckoff, S., Heyd, R. S., & Fox, R. 1999, ApJ, 512, L73
Wyckoff, S., & Theobald, J. 1989, Adv. Space Res., 9(3), 157
Yung, Y. L., & DeMore, W. B. 1999, Photochemistry of Planetary Atmospheres (New York: Oxford Univ. Press)